

Original Article

Citraconate promotes the malignant progression of colorectal cancer by inhibiting ferroptosis

Zongjiong Mai*, Yanyu Li*, Lei Zhang#, Hongyu Zhang#

The Fifth Affiliated Hospital of Sun Yat-sen University, Zhuhai, Guangdong, China. *Co-first authors. #Co-senior authors.

Received March 7, 2024; Accepted May 24, 2024; Epub June 15, 2024; Published June 30, 2024

Abstract: Metastasis is a principal factor in the poor prognosis of colorectal cancer. Recent studies have found microbial metabolites regulate colorectal cancer metastasis. By analyzing metabolomics data, we identified an essential fecal metabolite citraconate that potentially promotes colorectal cancer metastasis. Next, we tried to reveal its effect on colorectal cancer and the underlying mechanism. Firstly, the response of colorectal cancer cells (HCT116 and MC38 cells) to citraconate was assessed by Cell Counting Kit-8 assay, clonogenic assay, transwell migration and invasion assay. Moreover, we utilized an intra-splenic injection model to evaluate the effect of citraconate on colorectal cancer liver metastasis *in vivo*. Then molecular approaches were employed, including RNA sequencing, mass spectrometry-based metabolomics, western blot, quantitative real-time PCR, cell ferrous iron colorimetric assay and intracellular malondialdehyde measurement. *In vitro*, citraconate promotes the growth of colorectal cancer cells. *In vivo*, citraconate aggravated liver metastasis of colorectal cancer. Mechanistically, downstream genes of NRF2, NQO1, GCLC, and GCLM high expression induced by citraconate resulted in resistance to ferroptosis of colorectal cancer cells. In summary, citraconate promotes the malignant progression of colorectal cancer through NRF2-mediated ferroptosis resistance in colorectal cancer cells. Furthermore, our study indicates that fecal metabolite may be crucial in colorectal cancer development.

Keywords: Citraconate, colorectal cancer, malignant progression, ferroptosis

Introduction

Colorectal cancer is the third most common cancer and the second leading cause of cancer-related deaths worldwide [1]. Metastasis is a principal factor for the high mortality rate in patients with colorectal cancer [2]. Therefore, exploring the mechanism of metastasis is a feasible strategy to find more effective therapeutic targets for colorectal cancer. In recent years, more and more research reports suggest that intestinal flora metabolites play an essential role in the development of colorectal cancer [3, 4].

Intestinal flora can produce a variety of metabolites, such as short-chain carboxylate, which can not only directly act on the local intestine but also enter the systemic circulation to play a distant effect [5]. Studies have shown that patients with colorectal cancer and matched controls differ in the characteristics of fecal

metabolite composition [6, 7]. However, the role of different metabolites in colorectal cancer progression remains poorly understood.

Previous studies showed intestinal flora metabolites promote cancer progression through multiple mechanisms, including inducing DNA damage and genomic instability, influencing tumor inflammation and the host immune response [8], promoting tumor growth and angiogenesis [9]. Furthermore, harmful intestinal flora metabolites can promote colorectal cancer metastasis by influencing cell metabolism [10], inducing epigenetic modification of cells [11], and maintaining stemness [12]. Whether the metabolites of intestinal flora promote the malignant progression of colorectal cancer through other mechanisms remains to be further studied.

Herein, we analyzed the metabolic data of stool samples from patients with metastatic and non-metastatic colorectal cancer and found

Citraconate aggravates colorectal cancer progression

that the fecal samples of patients with metastatic colorectal cancer had higher level of citraconate. We speculated that citraconate may promote the malignant progression of colorectal cancer. In order to validate our speculation, we evaluate the effect of citraconate on the proliferation and metastasis of colorectal cancer *in vitro* and *in vivo*. Subsequently, we conducted RNA-seq and metabolomics to explore the underlying mechanisms and further investigated them through a series of molecular experiments.

Materials and methods

Cell culture and reagents

Human colorectal cancer cell lines HCT-116 and mouse colorectal cancer cell lines MC38 were originally derived at the Sun Yat-sen University Cancer Center (Guangzhou, China). The cell lines were cultivated with high glucose Dulbecco's modified eagle medium (DMEM, Gibco) supplemented with 10% fetal bovine serum in a humidified incubator (Thermo Fisher Scientific) with 5% CO₂ at 37°C. Citraconate (CAT#C82604) was purchased from Sigma-Aldrich. RSL3 (CAT#IR1120) and brusatol (CAT#IB0520) were purchased from Solarbio Life Science and Technology Ltd. Vancomycin hydrochloride (CAT#1404-93-9), ampicillin (CAT#69-52-3), metronidazole (CAT#443-48-1), and neomycin sulfate (CAT#1405-10-3) were purchased from Sangon Biotech.

Cell viability assay

Cell viability was assessed by the Cell Counting Kit-8 assay. Briefly, 3×10³ cells/well were seeded into 96-well plates. After the indicated treatments, Cell Counting Kit-8 solution (Beyotime Institute of Biotechnology, CAT#C0040) was added to the medium at a dilution of 1:10 and cells were incubated at 37°C for 2 h. Absorbance values were measured at 450 nm using a microplate reader.

Transwell assays

The migratory and invasive capacity of tumor cells were examined by a transwell chamber apparatus (24-well plates, 8-μm pore size. BD falcon, CAT#353097). For migration assays, HCT116 or MC38 cells in serum-free media were placed in the upper chamber, while medium containing 10% FBS was placed in the

lower chamber. For invasion experiments, HCT116 or MC38 cells in serum-free media were seeded into the hanging cell culture inserts coated with matrigel (Corning, CAT#356234), while medium containing 10% FBS was placed in the lower chamber. After 24 h, the cells were fixed, stained and photographed. Then, the average number of cells migrated to the lower chamber was counted in five fields at 100× magnification.

Colony formation assay

500 cells/well were seeded into a 6-well plate and treated with citraconate for 10 days. Cells were fixed in methanol and stained with crystal violet. The colonies were imaged by the camera and quantified.

Animal study

5 weeks C57 BL/6J female mice were purchased from SPF (Beijing) Biotechnology Co., Ltd. After 1 week of adaptive feeding, mice received daily gavage of combined antibiotics (vancomycin hydrochloride 100 mg/kg, ampicillin 200 mg/kg, metronidazole 200 mg/kg, and neomycin sulfate 200 mg/kg) for 5 days to deplete the gut microbiota [13]. After an interval of 2 days, the experimental group was fed with drinking water containing 3 mM citraconate for 3 days, and the control group was fed with sterile water. Further, after an abdominal injection of anesthesia, all the mice were established the colorectal cancer liver metastasis model by intrasplenic injection [14]. After that, mice in the control group were fed with sterile water, while mice in the experimental group continued to be fed with drinking water containing 3 mM citraconate. 8 days later, the mice's body, liver, and spleen were weighed, and photos were taken.

The animal experiments were approved by the animal ethics committee of The Fifth Affiliated Hospital of Sun Yat-sen University (Approval number: 00421).

RNA sequencing

RNA purification, reverse transcription, library construction and sequencing were performed at Shanghai Majorbio Bio-pharm Biotechnology Co., Ltd. (Shanghai, China). The data were analyzed on the free online platform of Majorbio Cloud Platform [15].

Citraconate aggravates colorectal cancer progression

Non-targeted liquid chromatography-mass spectrometry (LC-MS)-based metabolomics

After treatment with or without citraconate in HCT116 cells for 24 h, the control group cells (n=3) and citraconate-treated cells (n=3) were collected for LC-MS based non-targeted metabolomics analysis. LC-MS based non-targeted metabolomics analysis was performed at Shanghai Majorbio Bio-pharm Biotechnology Co., Ltd. (Shanghai, China). The data were analyzed on the free online platform of majorbio cloud platform [15]. The Orthogonal Partial Least-Squares-Discriminant Analysis (OPLS-DA) was utilized to distinguish the metabolites that differed between groups. The fold change (FC), Variable Importance of Projection (VIP) value and P value were used to screen the differential metabolites as follows: VIP>1 from the OPLS-DA models, P value <0.05 and $|\log_2FC|>1$.

Quantitative real-time PCR (qRT-PCR)

Total RNA was isolated from samples using a MolPure[®] Cell/Tissue Total RNA Kit (YEASEN, CAT#19221ES50) according to the manufacturer's instructions. RNA was reverse transcribed using a Hifair[®] III 1st Strand cDNA Synthesis SuperMix for qPCR (gDNA digester plus) Kit (YEASEN, CAT#11141ES60) and qPCR was performed on the cDNA using Hieff[®] qPCR SYBR Green Master Mix (Low Rox Plus) Kit (YEASEN, CAT#11202ES08) and gene-specific primers (Table S1). The following PCR conditions were used: 40 cycles of denaturation at 95°C for 10 s, annealing/elongation at 60°C for 30 s.

Western blotting assay

Cells were lysed using RIPA buffer (Beyotime Institute of Biotechnology, CAT#P0013) with 1% PMSF (Beyotime Institute of Biotechnology, CAT#ST506), and the lysates were centrifuged at 12,000 g at 4°C for 10 min. The BCA Protein Assay Kit (Beyotime Institute of Biotechnology, CAT#P0012) was employed to quantify the protein concentration. For Western blotting analysis, the same amounts of samples were separated by SDS-PAGE gel electrophoresis and transferred to a PVDF membrane. After incubation with a protein-free rapid blocking buffer (Servicebio, CAT#G2052) for 10 minutes, the membrane was incubated at 4°C overnight

with the corresponding primary antibody. The primary antibodies used in the present study are NQO1 rabbit polyAb (Beyotime Institute of Biotechnology, CAT#AF7614, 1:2000), GCLC rabbit polyAb (Beyotime Institute of Biotechnology, CAT#AF6969, 1:1000), GCLM rabbit polyAb (Beyotime Institute of Biotechnology, CAT#AF6972, 1:1000), NRF2 rabbit polyAb (Beyotime Institute of Biotechnology, CAT#AF7623, 1:1000), KEAP1 mouse polyAb (Proteintech, CAT#60027-1-Ig, 1:1000) and recombinant anti-GAPDH antibody (HRP Conjugated) (Servicebio, CAT#ZB15004-HRP-100, 1:3000). After washing, the membranes were incubated with corresponding HRP-conjugated secondary antibodies for 1 hour at room temperature, HRP-conjugated goat anti-rabbit secondary antibody (TransGen Biotech, CAT#HS101-01, 1:5000) for NQO1, GCLC, GCLM, NRF2. And HRP-conjugated goat anti-mouse secondary antibody (TransGen Biotech, CAT#HS201-01, 1:5000) for KEAP1. The electrochemiluminescence (ECL) reagent (Thermo Fisher Scientific, 34580) was used to detect target bands and capture the image. The quantitative analysis was performed using ImageJ software.

Cell ferrous iron colorimetric assay

The intracellular relative ferrous iron level was assessed using a Cell Ferrous Iron Colorimetric Assay Kit (Elabscience, CAT#E-BC-K881-M). 2×10^6 cells were harvested and lysed on ice for 10 min with 200 μ L of lysis buffer before being centrifuged at 15,000 g for 10 min to collect the supernatant. Then, the ferrous iron level was assessed according to the manufacturer's instructions.

Intracellular malondialdehyde (MDA) measurement

The intracellular relative MDA level was measured using the malondialdehyde (MDA) assay kit (Beyotime Institute of Biotechnology, CAT#S0131M). 5×10^6 cells were harvested and lysed on ice for 10 min with 100 μ L of lysis buffer before being centrifuged at 12,000 g for 10 min to collect the supernatant. Then, the intracellular MDA level was assessed following the procedure recommended by the manufacturer. The accurate calculation of MDA was based on the total amount of protein in each sample, which was tested using the BCA protein assay

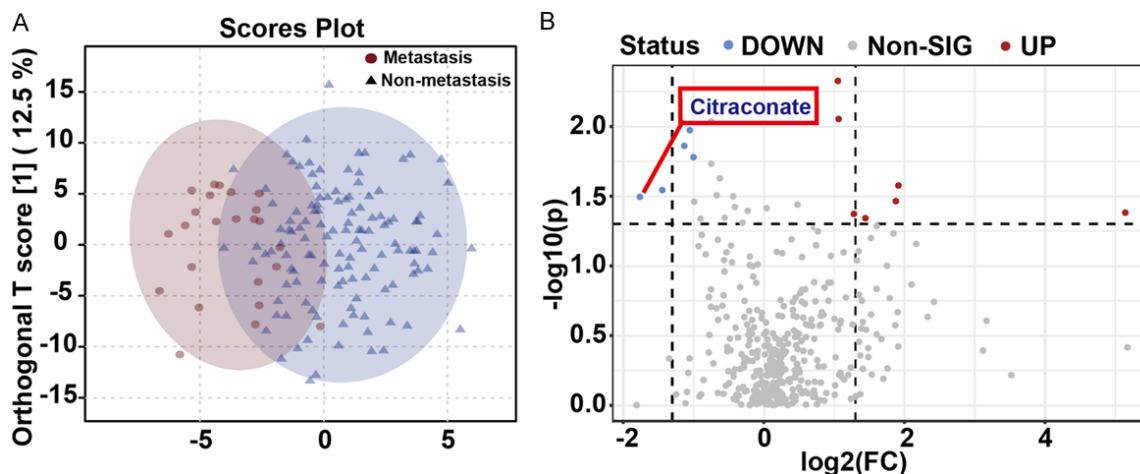


Figure 1. Citraconate potentially promotes the malignant progression of colorectal cancer. A. OPLS-DA model of fecal metabolites. B. Volcano plot analysis of fecal metabolites in patients with non-metastatic and metastatic colorectal cancer ($P < 0.05$, $VIP > 1$). Non-SIG: Non-significant.

kit (Beyotime Institute of Biotechnology, CAT#P0012).

Statistical analysis

Statistical analyses were performed using GraphPad Prism 8.0. The results are expressed as Mean \pm SEM. Unpaired two-tailed Student's *t* test was used for comparisons between the two groups. *P* value < 0.05 was considered to be statistically significant, marking with * $P < 0.05$, ** $P < 0.01$, *** $P < 0.005$, **** $P < 0.001$. Experiments were repeated at least three times.

Results

Citraconate potentially promotes the malignant progression of colorectal cancer

We analyzed the fecal metabolomics data of patients with metastatic and non-metastatic colorectal cancer [16] by using the MetaboAnalyst 5.0 (<https://www.metaboanalyst.ca/home.xhtml>) online analysis software and found that the metabolite composition of the two groups was different (Figure 1A). And the level of citraconate was higher in fecal samples from patients with metastatic colorectal cancer (Figure 1B).

Citraconate promotes the development of colorectal cancer

In order to indicate the effect of citraconate on cancer cells, we first treated HCT116 and

MC38 cells with citraconate *in vitro*. We found that citraconate significantly promotes colorectal cancer cell proliferation (Figure 2A, 2B) and clonal formation (Figure 2C-F). Moreover, citraconate notably facilitates colorectal cancer cell migration (Figure 3A-D) and invasion (Figure 3E-H). Further, we detected the impact of citraconate on colorectal cancer *in vivo*. After injecting the same amounts of MC38 cells into the spleen, the results suggested that citraconate did not affect body weight (Figure 4A), and promoted liver metastasis of colorectal cancer in mice (Figure 4B-D). Compared with the control group, the liver metastasis in the citraconate group mice was more severe (Figure 4C). As for the weight of the liver metastatic tumors, a similar trend was observed between the control group and the citraconate group (Figure 4B). And H&E staining of livers sections revealed a higher number of liver metastases (black arrow) in the citraconate group (Figure 4D). Both *in vivo* and *in vitro* evidence confirmed that citraconate promotes the malignant progression of colorectal cancer.

Citraconate potentially inhibits ferroptosis

In order to further investigate the mechanism of citraconate promoting the malignant progression of colorectal cancer, RNA-seq and metabolomics were performed on HCT116 cells treated with citraconate. RNA-seq results showed that the expression of ferroptosis suppressor genes [17], *NQO1*, *GCLC*, and *GCLM*

Citraconate aggravates colorectal cancer progression

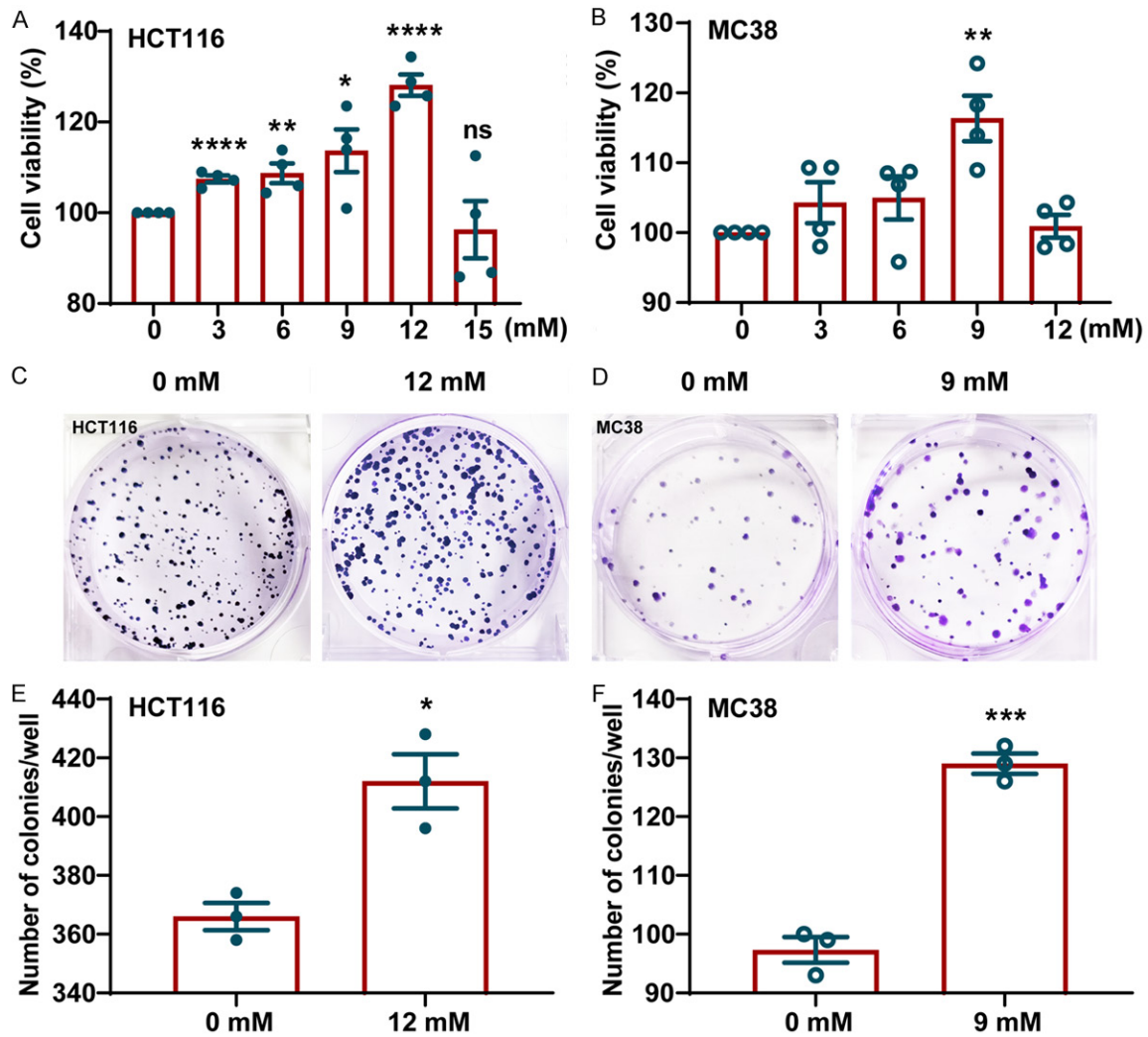


Figure 2. Citraconate promotes the proliferation and clonal formation of colorectal cancer cells. A, B. HCT116 and MC38 cells were incubated with various concentrations of citraconate for 48 hours, and cell proliferation was detected for 48 hours by the Cell Counting Kit-8 assay. C, D. Representative images of cell colonies. E, F. The bar graph shows the quantification of colony numbers. Experiments were repeated at least three times. Unpaired two-tailed Student's *t* test was used to compare the two groups. Data were presented as Mean \pm SEM. ns stands for no significance. **P*<0.05, ***P*<0.01, ****P*<0.005, *****P*<0.001.

was significantly up-regulated (Figure 5A). KEGG annotation of differential expression genes was most significantly enriched in cell growth and death pathways (Figure 5B). Gene-set enrichment analysis of transcripts hinted that citraconate may regulate ferroptosis in colorectal cancer cells (Figure 5C). Using OPLS-DA models to explore differences in cell metabolic phenotypes, the separation of the treatment group and the control group in positive (Figure S1A) and negative (Figure S1B) ion mode was apparent, along with model characteristics. Cluster analysis of differential metabolites showed that the contents of glutamic

acid and glutamine decreased in the cancer cells treated with citraconate (Figure S1C). Meanwhile, γ -glutamyl peptide increased in the treatment group (Figure S1D). KEGG topological analysis based on differential metabolites revealed that the alanine, aspartate, and glutamate metabolic pathways are the most important (Figure S1E).

Citraconate promotes the malignant progression of colorectal cancer by suppressing ferroptosis

To further clarify the mechanism of citraconate accelerating the malignant progression of

Citraconate aggravates colorectal cancer progression

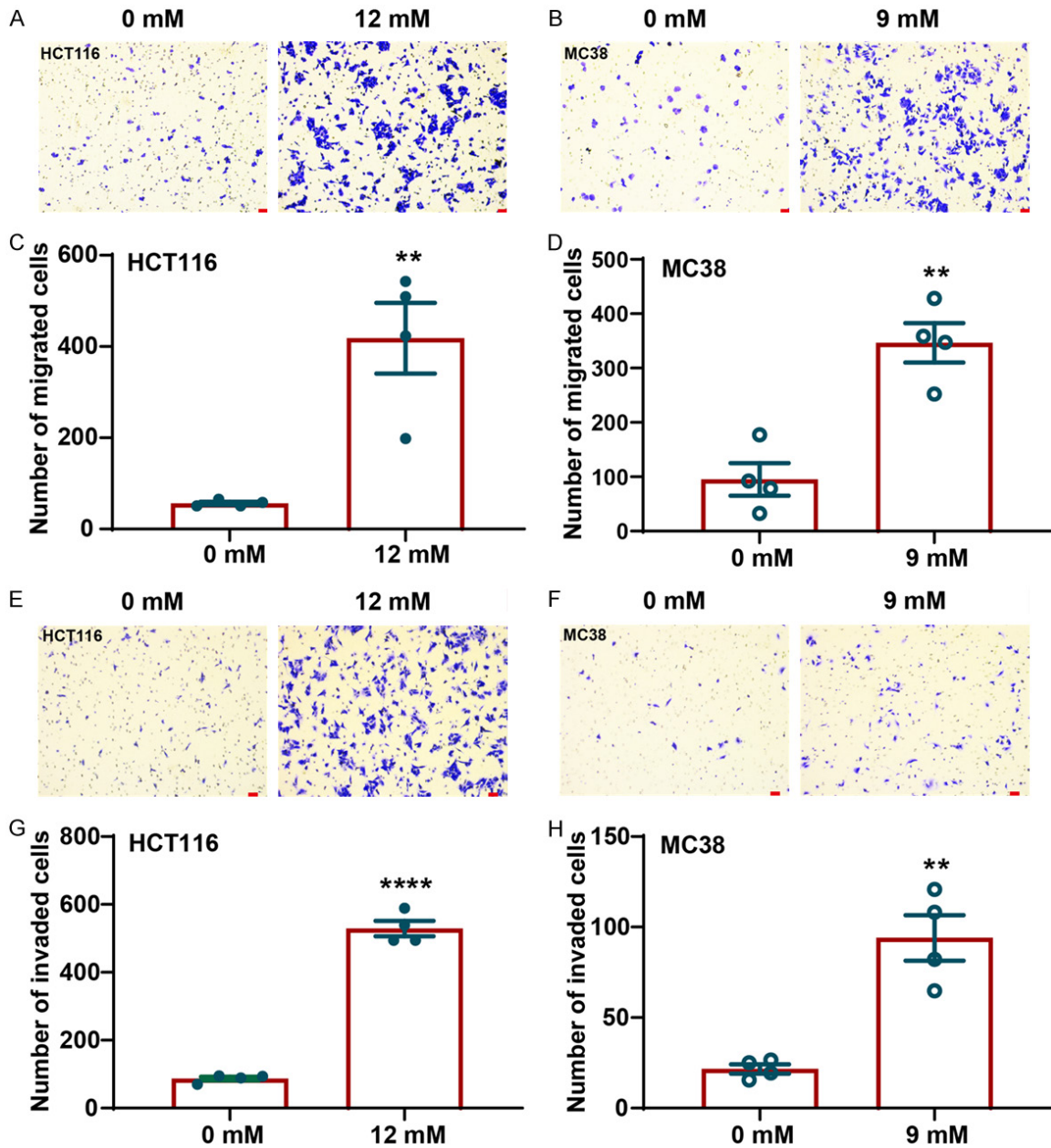


Figure 3. Citraconate promotes colorectal cancer cell migration and invasion. For migration assays, 7.5×10^5 HCT116 and 2.8×10^5 MC38 cells were stimulated with 12 mM and 9 mM citraconate for 24 hours, respectively. For invasion experiments, 1×10^6 HCT116 or 3.3×10^4 MC38 cells were treated with 12 mM and 9 mM citraconate for 24 hours, respectively. Representative images of migrating cells (A, B) and invading cells (E, F) stained with crystal violet were displayed. Scale bars: 50 μ m in red. Quantitative analysis for the number of migrating cells (C, D) and invading cells (G, H). Experiments were repeated at least three times. Unpaired two-tailed Student's *t* test was used for comparisons between the two groups. Data were presented as Mean \pm SEM. ***P*<0.01, *****P*<0.001.

colorectal cancer cells, we treated HCT116 and MC38 cells with citraconate *in vitro*. The results indicated that the mRNA and protein expression of ferroptosis suppressor genes *NQO1* (Figure 6A, 6D, 6G), *GCLC* (Figure 6B, 6E, 6H) and *GCLM* (Figure 6C, 6F, 6I) are significantly up-regulated in HCT116 cells. Similarly, the

mRNA and protein expression of *NQO1* (Figure S2A, S2D, S2G), *GCLC* (Figure S2B, S2E, S2H) and *GCLM* (Figure S2C, S2F, S2I) are also significantly up-regulated in MC38 cells. To further investigate whether citraconate regulates ferroptosis in colorectal cancer cells, we tested the intracellular relative ferrous iron and MDA

Citraconate aggravates colorectal cancer progression

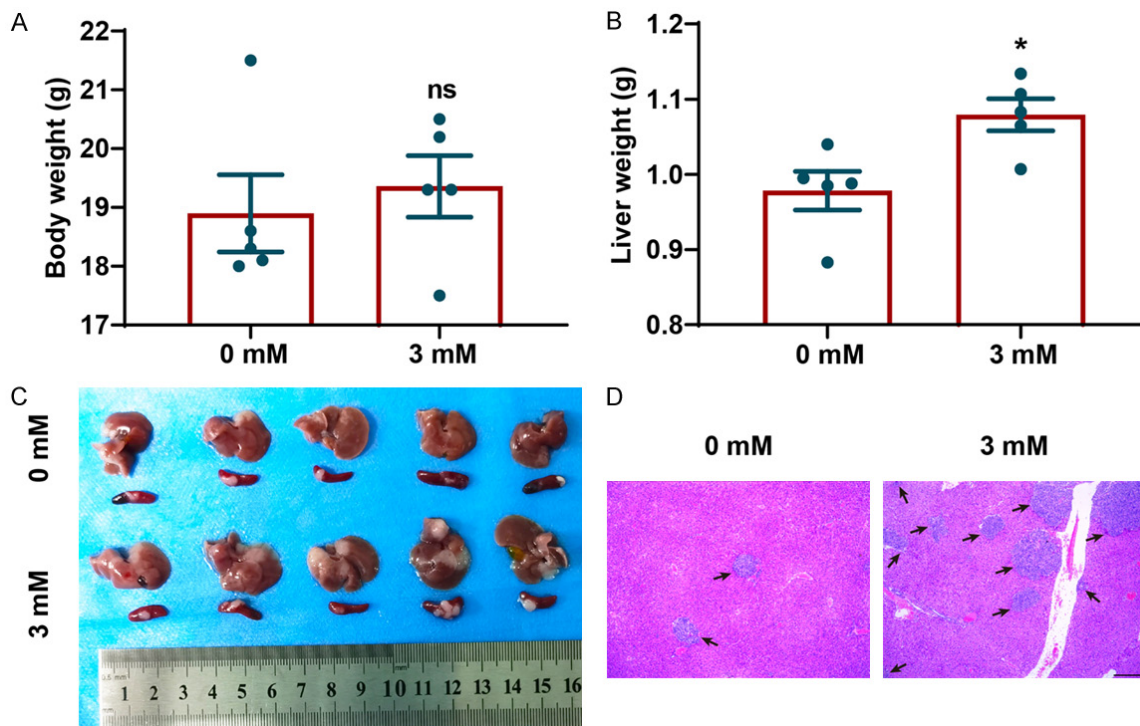


Figure 4. Citraconate promotes liver metastasis of colorectal cancer. Weights of whole body (A) and liver (B) in the control group (n=5) and citraconate group (n=5) were measured. (C) Imaging of liver and spleen specimens from metastatic models established by spleen injection of MC38 cells. (D) Hepatic H&E staining of mouse liver with liver metastases. Scale bars: 250 μm in black. Unpaired two-tailed Student's *t* test was used for comparisons between the two groups. Data were presented as Mean ± SEM. ns stands for no significance. *P<0.05.

levels. The data illustrated that both of them in the citraconate treatment group decrease remarkably in HCT116 and MC38 cells (Figure 7A, 7B).

To determine whether citraconate promotes the malignant progression of colorectal cancer via inhibiting ferroptosis, the ferroptosis inducer RSL3 was introduced. RSL3 increased the intracellular relative MDA and ferrous iron levels in HCT116 (Figure S3A, S3C) and MC38 (Figure S3B, S3D) cells, which were attenuated by citraconate. As shown in Figure 7, citraconate promoted HCT116 cells proliferation (Figure 7C) and migration (Figure 7D, 7E), which were attenuated by RSL3. Meanwhile, as shown in Figure S4, similar results were found in MC38 cells. All these findings indicated that citraconate induces malignant progression of colorectal cancer by inhibiting ferroptosis.

Citraconate inhibits ferroptosis by upregulating NRF2 protein level

Previous studies reported that ferroptosis suppressor genes *GCLC*, *GCLM* and *NQO1* are

NRF2 downstream genes [18]. Herein, we detected the level of NRF2 mRNA and protein, and found that citraconate only markedly up-regulates NRF2 protein level (Figure 8B, 8C), rather than mRNA (Figure 8A). Meanwhile, citraconate did not affect the KEAP1 (Kelch-like ECH-associated protein 1) protein level (Figure 8B, 8C). Then, we treated colorectal cancer cells with brusatol, which induces NRF2 depletion through KEAP1-independent [19], and found that citraconate-induced cell proliferation (Figure 8D) and migration (Figure 8E, 8F) were attenuated by brusatol. All these results indicated that citraconate induces malignant progression of colorectal cancer through inhibiting ferroptosis by increasing NRF2 protein level.

Discussion

Fecal metabolites between patients with colorectal cancer and matched controls have different composition characteristics [6, 7]. However, there is little research on the roles and mechanisms of these differential metabo-

Citraconate aggravates colorectal cancer progression

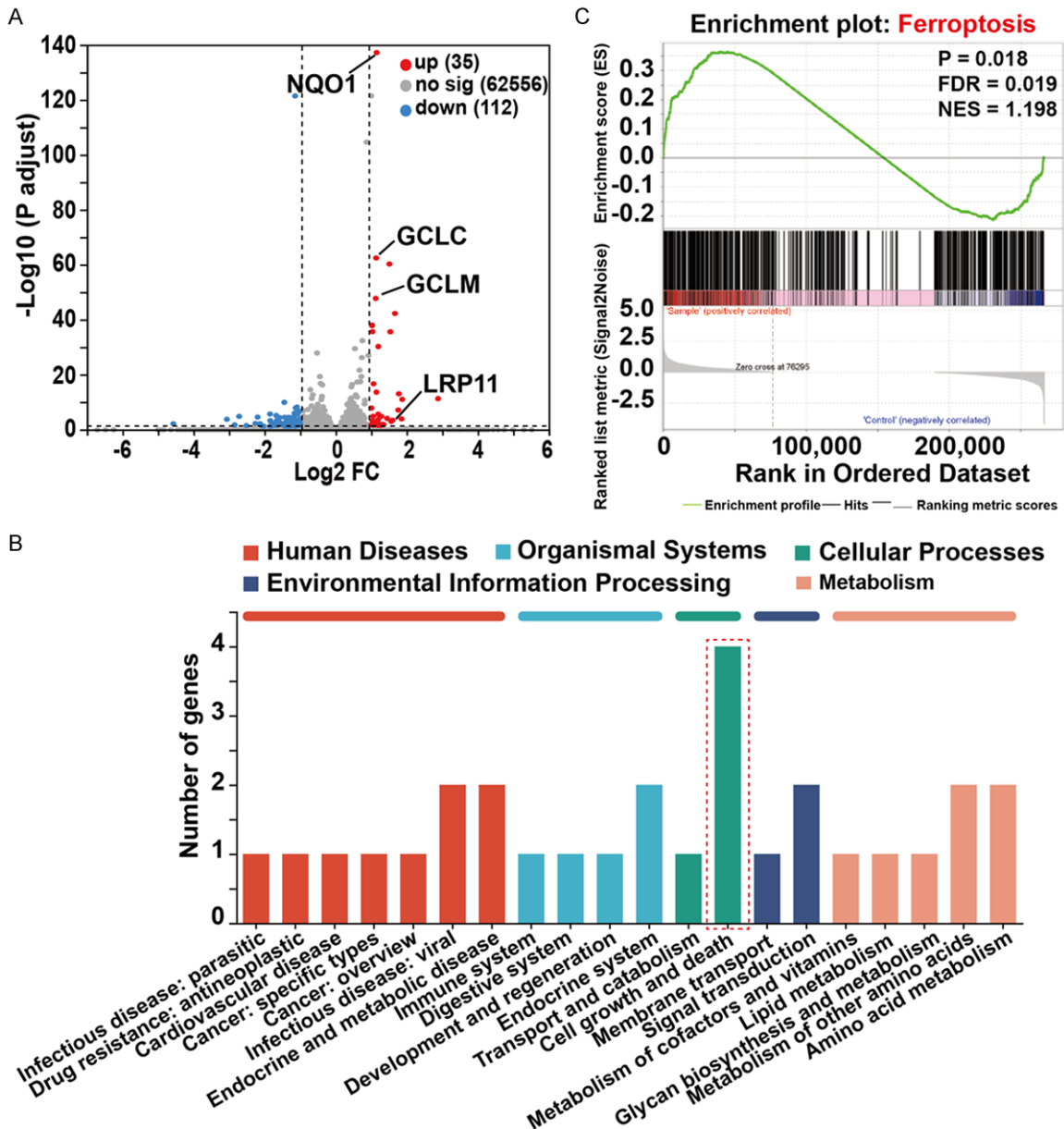


Figure 5. Citraconate potentially inhibits ferroptosis in colorectal cancer cells. RNA-seq was performed on HCT116 cells treated with 12 mM citraconate for 24 hours. A. The volcano plot showed the differential expression genes between the citraconate group (n=3) and the control group (n=3). B. The bar graph shows the KEGG annotation of differential expression genes. C. Gene set enrichment analysis of transcripts.

lites in the progression of colorectal cancer. Herein, we found that the level of citraconate was higher in fecal samples from patients with metastatic colorectal cancer (**Figure 1**). Citraconate widely distributes in various tissue and biofluids [20] and possesses multifaceted features such as anti-inflammatory, anti-oxidative and antiviral properties [21]. According to a previous report, citraconate is elevated in the serum of colorectal cancer patients with dis-

ease progression status [22]. Therefore, two questions were raised regarding (1) the function of citraconate in colorectal cancer progression and (2) the mechanism by which citraconate affects colorectal cancer progression.

In order to identify the correlations between citraconate and colorectal cancer progression, two colorectal cancer cell lines (HCT116 and MC38) were treated with exogenous citracon-

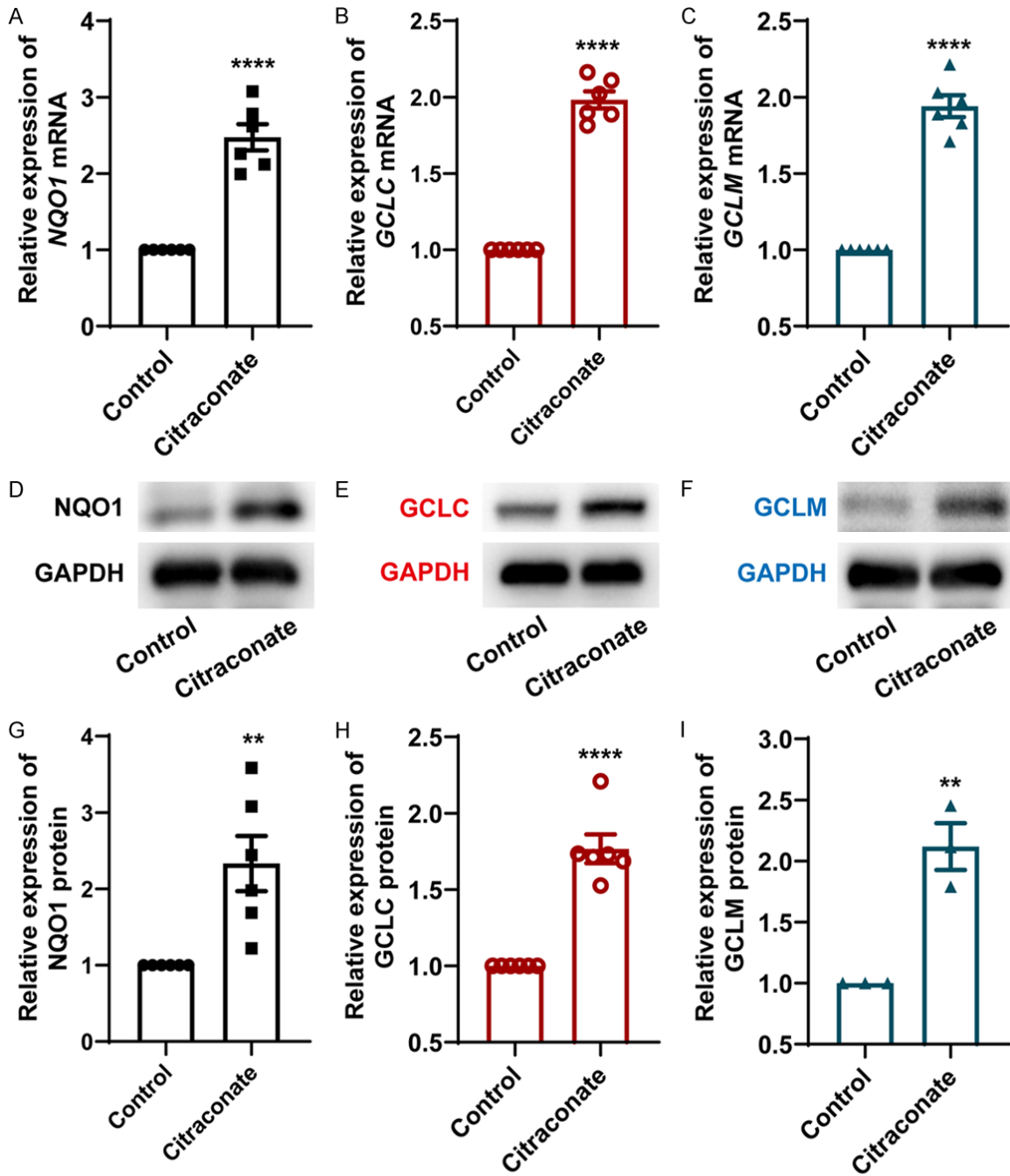


Figure 6. Citraconate up-regulates the expression of ferroptosis suppressor genes. *NQO1* (A), *GCLC* (B), and *GCLM* (C) mRNA were detected by qRT-PCR after HCT116 cells were treated with 12 mM citraconate for 24 hours. Protein expression of *NQO1* (D, G), *GCLC* (E, H), and *GCLM* (F, I) was detected by western blot after HCT116 cells were treated with 12 mM citraconate for 48 hours. Experiments were repeated at least three times. Unpaired two-tailed Student's *t* test was used for comparisons between the two groups. Data were presented as Mean \pm SEM. *P<0.05, **P<0.01, ***P<0.005, ****P<0.001.

ate, respectively (Figures 2 and 3). Meanwhile, an intra-splenic injection model was used to evaluate the effect of citraconate on colorectal cancer liver metastasis *in vivo* (Figure 4). Both

in vivo and *in vitro* evidence confirmed that citraconate promotes the proliferation and metastasis of colorectal cancer cells (malignant progression). Moreover, whether colorec-

Citraconate aggravates colorectal cancer progression

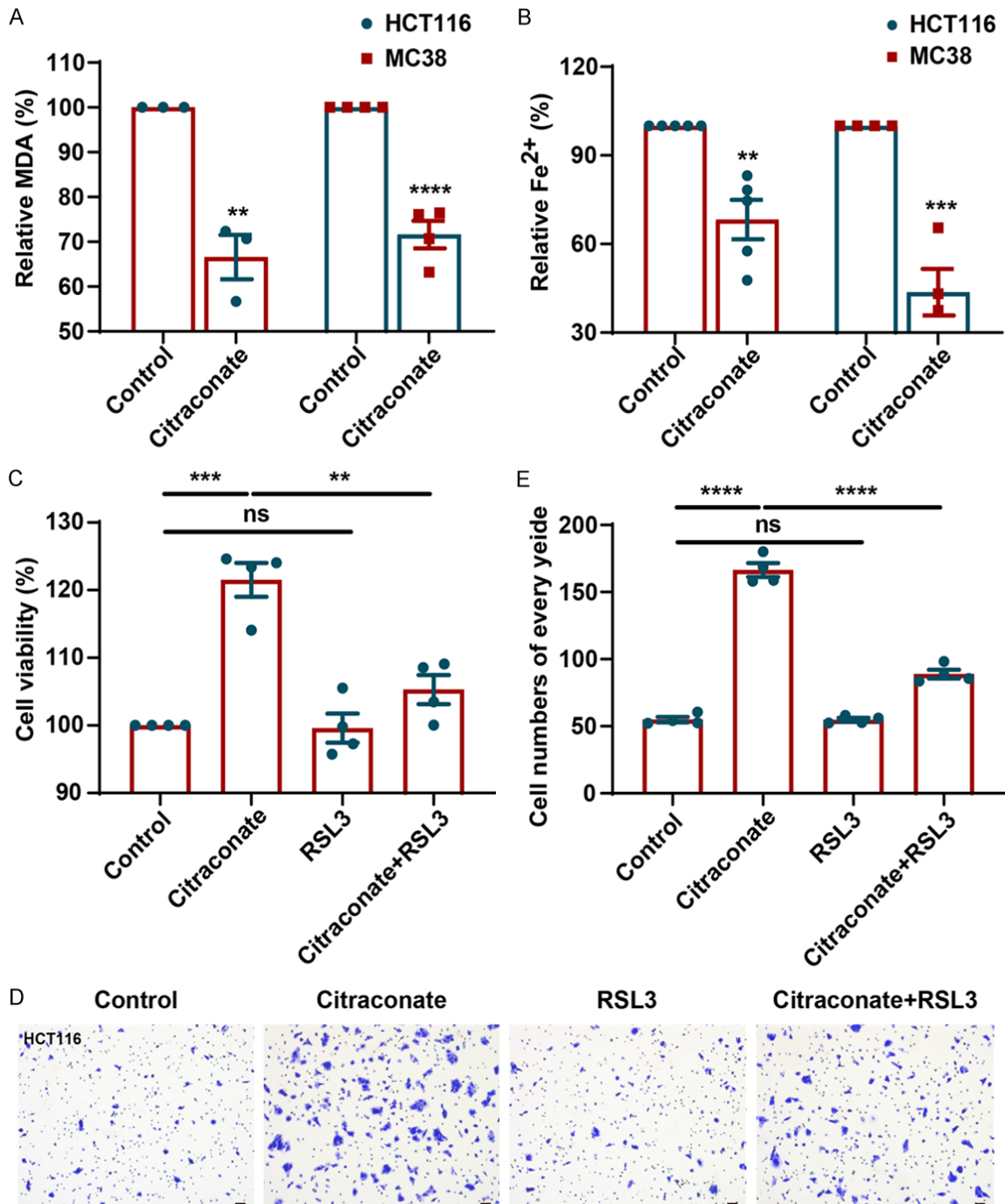


Figure 7. Citraconate inhibits ferroptosis in colorectal cancer cells. HCT116 cells were treated with 12 mM citraconate for 72 hours, and MC38 cells were stimulated with 9 mM citraconate for 48 hours. The cellular MDA (A) and ferrous iron (B) levels were assessed. (C) HCT116 cells were incubated with 12 mM citraconate with or without 3 μ M RSL3 for 48 hours. Then, cell viability was measured by Cell Counting Kit-8 assay. After 7.5×10^5 HCT116 cells seeded in the transwell chamber for 6 hours, the cells were pre-treated with 1 μ M RSL3 for 2 hours. Next, treatment groups were incubated with 12 mM citraconate, 1 μ M RSL3, or both of them for 16 hours, respectively. (D) Representative images of migrating cells stained with crystal violet were displayed. Scale bars: 50 μ m in black. (E) Quantitative analysis for the number of migrating cells. Experiments were repeated at least three times. Unpaired two-tailed Student's *t* test was used for comparisons between the two groups. Data were presented as Mean \pm SEM. ns stands for no significance. ***P*<0.01, ****P*<0.005, *****P*<0.001.

Citraconate aggravates colorectal cancer progression

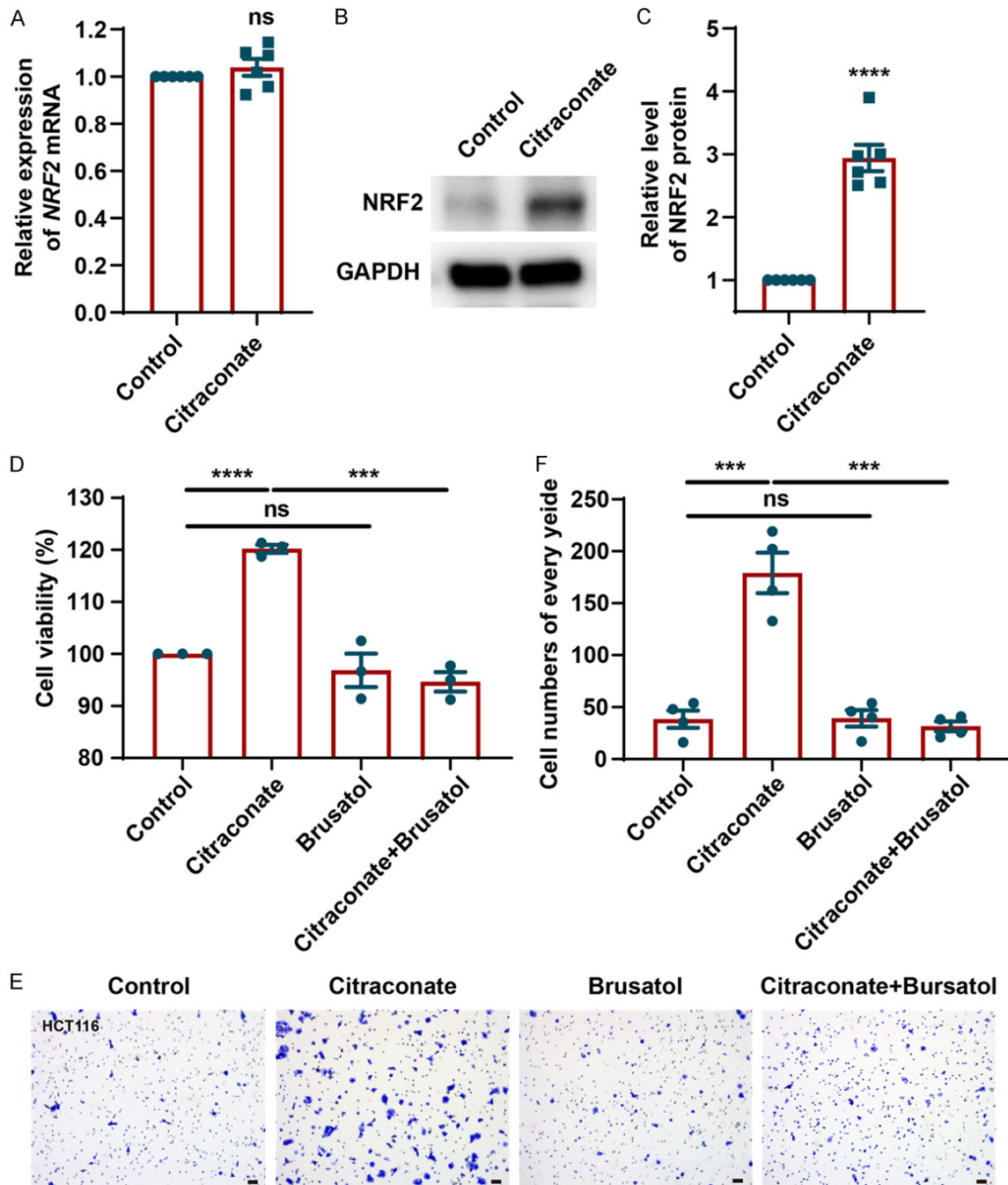


Figure 8. Citraconate inhibits ferroptosis by upregulating NRF2 protein level. A. NRF2 mRNA was detected by qRT-PCR after HCT116 cells treated with 12 mM citraconate for 24 hours. B, C. The protein level of NRF2 and KEAP1 was detected by western blot after HCT116 cells were stimulated with 12 mM citraconate for 48 hours. D. HCT116 cells were incubated with 12 mM citraconate with or without 5 nM brusatol for 48 hours. Then, cell viability was accessed by Cell Counting Kit-8 assay. The cells were pre-treated with 5 nM brusatol for 2 hours after 7.5×10^5 HCT116 cells were seeded in the transwell chamber for 6 hours. Subsequently, treatment groups were incubated with 12 mM citraconate, 5 nM brusatol, or both of them for 16 hours, respectively. E. Representative images of migrating cells stained with crystal violet were displayed. Scale bars: 50 μ m in black. F. Quantitative analysis for the number of migrating cells. Experiments were repeated at least three times. Unpaired two-tailed Student's *t* test was used for comparisons between the two groups. Data were presented as Mean \pm SEM. ns means no significance. ****P*<0.005, *****P*<0.001.

tal cancer patients with poor prognosis have a higher level of citraconate in their feces is necessary to analyze in the following study.

To further explore the underlying mechanism of citraconate, which is involved in the malignant progression of colorectal cancer, RNA-seq and metabolomics were performed. RNA-seq data showed that citraconate enhances the expression of *NQO1*, *GCLC*, and *GCLM* (**Figure 5**), which are ferroptosis suppressor genes [17]. Furthermore, we verified that the mRNA and protein of these genes of colorectal cancer cells were significantly up-regulated in the citraconate treatment group *in vitro* (**Figures 6 and S2**). Meanwhile, metabolomics data suggested that intracellular γ -glutamyl peptide increases in the citraconate treatment group (**Figure S1**), which has been reported to inhibit ferroptosis [23]. Ferroptosis is a new form of cell death discovered recently and mainly results from intracellular ferrous iron accumulation and lipid peroxidation [24]. It is known that excessive iron promotes the overproduction of reactive oxygen species by the Fenton reaction, which leads to cell cytotoxicity [25] and is responsible for ferroptosis [26]. Lipid peroxidation is a key event of ferroptosis [27], and MDA is the principal and most studied byproduct of lipid peroxidation [28]. In our study, we found that citraconate markedly suppresses the level of cellular MDA (**Figure 7A**) and ferrous iron (**Figure 7B**) in colorectal cancer cells. These findings confirmed that citraconate inhibits ferroptosis of colorectal cancer.

Increasing studies show that inhibiting ferroptosis can promote the malignant progression of colorectal cancer and treatment resistance [29, 30]. Inhibition of ferroptosis can promote tumor invasion and metastasis through multiple mechanisms, such as affecting lipid metabolism of tumor cells [31], promoting epithelial-mesenchymal transition of cancer cells [32, 33], inhibiting cancer stem cells' growth [34], and so on. Combining our findings, we speculate that citraconate may lead to malignant progression of colorectal cancer by inhibiting ferroptosis. *NQO1*, *GCLC*, and *GCLM* are critical proteins involved in glutathione synthesis [35, 36], and glutathione acts as a necessary cofactor for the normal function of glutathione peroxidase 4 (GPX4), which is the critical enzyme for oxidative lipid homeostasis and ferroptosis [37]. GPX4 acts as a bulwark against lipid

peroxidation, and its inhibition could trigger ferroptosis [38]. In order to find out the relationship between ferroptosis and colorectal cancer malignant progression induced by citraconate. RSL3, a GPX4 inhibitor, which covalently binds to its selenocysteine residue (Sec46) and induces cell ferroptosis [39], was introduced in this study. RSL3 has used as a ferroptosis inducer for colorectal cancer cells in previous studies [40-42]. Herein, we also found that RSL3 increased the intracellular relative ferrous iron and MDA levels in HCT116 and MC38 cells. And expectedly, RSL3-induced ferroptosis could be attenuated by citraconate (**Figure S3**). Our results suggested that citraconate-induced colorectal cancer malignant progression (**Figures 7 and S4**) were attenuated by RSL3. These findings confirmed that citraconate promotes the malignant progression of colorectal cancer by inhibiting ferroptosis.

Previous studies showed that NRF2 translocates into the nucleus and interacts with antioxidant response element (ARE), driving the downstream gene expression, such as *GCLC*, *GCLM*, and *NQO1* [43]. Chen et al. reported that citraconate exerted a stabilizing effect on NRF2 in human keratinocyte cells (HaCaT) and induced transcription of downstream factors of NRF2 [21]. Similarly, this study found that citraconate apparently increases NRF2 protein level (**Figure 8B, 8C**) rather than mRNA (**Figure 8A**) in HCT116 cells. NRF2 is an essential negative regulator of ferroptosis, making it a vital candidate to mediate ferroptosis inhibition effects, and has become a key target in the development of anti-cancer therapies [44]. Next, to find out the relationship between NRF2 and the malignant progression of colorectal cancer induced by citraconate, we introduced brusatol which induces NRF2 depletion [19]. The results suggested that citraconate-induced cell proliferation (**Figure 8D**) and migration (**Figure 8E, 8F**) were attenuated by brusatol. Thus, citraconate functions as a ferroptosis inhibitor mainly via up-regulating of NRF2 protein level. However, the mechanism of citraconate blocking the degradation of NRF2 needs further investigation. Citraconate has two naturally occurring isomers, namely itaconate and mesaconate, which differ from it only by the position of a double bond [20, 21]. And citraconate is the strongest electrophile and SH-alkylator among the three isomers [21].

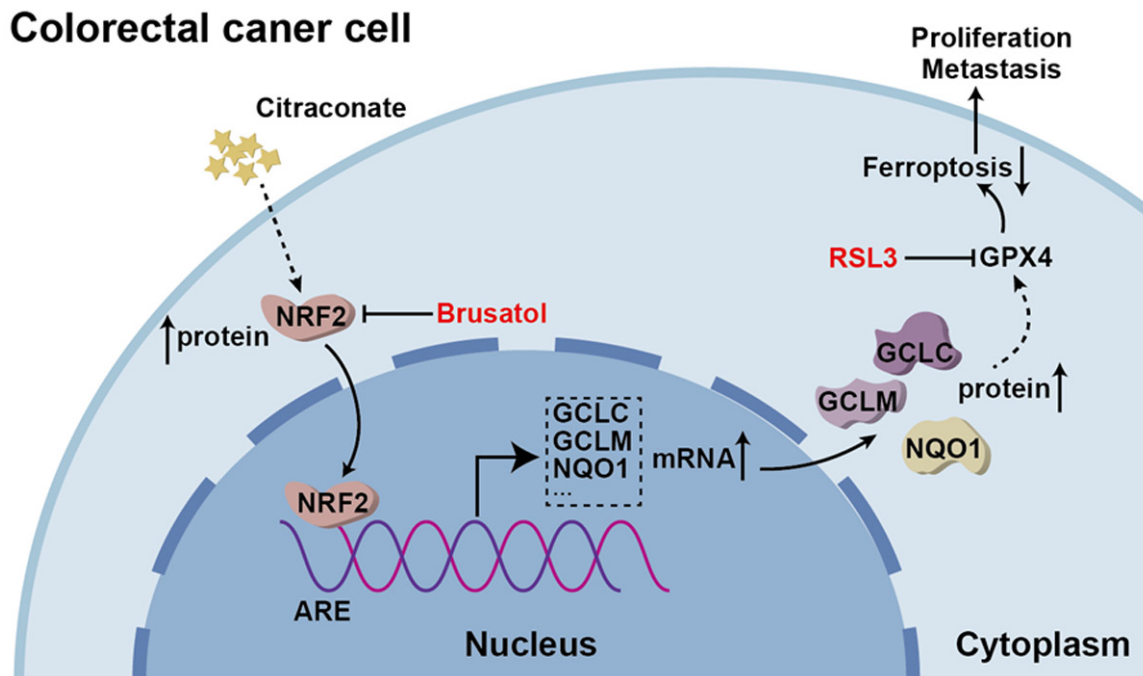


Figure 9. Citraconate promotes the malignant progression of colorectal cancer through NRF2-mediated ferroptosis resistance in colorectal cancer cells.

Furthermore, itaconate activates NRF2 by alkylation of KEAP1 cysteine residues [45]. In this study, we found that citraconate did not affect the KEAP1 protein level. Based on these clues, we consider that citraconate may activate NRF2 through alkylation of KEAP1, similar to itaconate.

In summary, in this study, we found that citraconate promotes the malignant progression of colorectal cancer through NRF2-mediated ferroptosis resistance in colorectal cancer cells (Figure 9).

Disclosure of conflict of interest

None.

Abbreviations

LC-MS, liquid chromatography-mass spectrometry; OPLS-DA, Orthogonal Partial Least-Squares-Discriminant Analysis; FC, Fold change; VIP, Variable Importance of Projection; MDA, Malondialdehyde; GPX4, Glutathione Peroxidase 4; NQO1, NAD(P)H quinone oxidoreductase 1; NRF2, Nuclear factor erythroid 2-related factor 2; GCLC, glutamate-cysteine ligase, catalytic subunit; GCLM, glutamate-cys-

teine ligase, modifier subunit; KEAP1, Kelch-like ECH-associated protein 1.

Address correspondence to: Lei Zhang and Hongyu Zhang, The Fifth Affiliated Hospital of Sun Yat-sen University, Zhuhai, Guangdong, China. E-mail: zhangl92@sysu.edu.cn (LZ); zhhyu@mail.sysu.edu.cn (HYZ)

References

- [1] Sung H, Ferlay J, Siegel RL, Laversanne M, Soerjomataram I, Jemal A and Bray F. Global cancer statistics 2020: GLOBOCAN estimates of incidence and mortality worldwide for 36 cancers in 185 countries. *CA Cancer J Clin* 2021; 71: 209-249.
- [2] Fakih MG. Metastatic colorectal cancer: current state and future directions. *J Clin Oncol* 2015; 33: 1809-1824.
- [3] Niekamp P and Kim CH. Microbial metabolite dysbiosis and colorectal cancer. *Gut Liver* 2023; 17: 190-203.
- [4] Kim M, Vogtmann E, Ahlquist DA, Devens ME, Kisiel JB, Taylor WR, White BA, Hale VL, Sung J, Chia N, Sinha R and Chen J. Fecal metabolomic signatures in colorectal adenoma patients are associated with gut microbiota and early events of colorectal cancer pathogenesis. *mBio* 2020; 11: e03186-19.

- [5] Cong J, Zhou P and Zhang R. Intestinal microbiota-derived short chain fatty acids in host health and disease. *Nutrients* 2022; 14: 1977.
- [6] Sinha R, Ahn J, Sampson JN, Shi J, Yu G, Xiong X, Hayes RB and Goedert JJ. Fecal microbiota, fecal metabolome, and colorectal cancer interrelations. *PLoS One* 2016; 11: e0152126.
- [7] Weir TL, Manter DK, Sheflin AM, Barnett BA, Heuberger AL and Ryan EP. Stool microbiome and metabolome differences between colorectal cancer patients and healthy adults. *PLoS One* 2013; 8: e70803.
- [8] Yoshimoto S, Loo TM, Atarashi K, Kanda H, Sato S, Oyadomari S, Iwakura Y, Oshima K, Morita H, Hattori M, Honda K, Ishikawa Y, Hara E and Ohtani N. Obesity-induced gut microbial metabolite promotes liver cancer through senescence secretome. *Nature* 2013; 499: 97-101.
- [9] Nasr R, Shamseddine A, Mukherji D, Nassar F and Temraz S. The crosstalk between microbiome and immune response in gastric cancer. *Int J Mol Sci* 2020; 21: 6586.
- [10] He Y, Ling Y, Zhang Z, Mertens RT, Cao Q, Xu X, Guo K, Shi Q, Zhang X, Huo L, Wang K, Guo H, Shen W, Shen M, Feng W and Xiao P. Butyrate reverses ferroptosis resistance in colorectal cancer by inducing c-Fos-dependent xCT suppression. *Redox Biol* 2023; 65: 102822.
- [11] Zhao Y, Wang C and Goel A. Role of gut microbiota in epigenetic regulation of colorectal cancer. *Biochim Biophys Acta Rev Cancer* 2021; 1875: 188490.
- [12] Ternes D, Tsenkova M, Pozdeev VI, Meyers M, Koncina E, Atatri S, Schmitz M, Karta J, Schmoetten M, Heinken A, Rodriguez F, Delbrouck C, Gaigneaux A, Ginolhac A, Nguyen TTD, Grandmougin L, Frachet-Bour A, Martin-Gallaussiaux C, Pacheco M, Neuberger-Castillo L, Miranda P, Zuegel N, Ferrand JY, Gantenbein M, Sauter T, Slade DJ, Thiele I, Meiser J, Haan S, Wilmes P and Letellier E. The gut microbial metabolite formate exacerbates colorectal cancer progression. *Nat Metab* 2022; 4: 458-475.
- [13] Li JH, Liu JL, Li XW, Liu Y, Yang JZ, Chen LJ, Zhang KK, Xie XL and Wang Q. Gut microbiota from sigma-1 receptor knockout mice induces depression-like behaviors and modulates the cAMP/CREB/BDNF signaling pathway. *Front Microbiol* 2023; 14: 1143648.
- [14] Ma X, Zhou Z, Zhang X, Fan M, Hong Y, Feng Y, Dong Q, Diao H and Wang G. Sodium butyrate modulates gut microbiota and immune response in colorectal cancer liver metastatic mice. *Cell Biol Toxicol* 2020; 36: 509-515.
- [15] Ren Y, Yu G, Shi C, Liu L, Guo Q, Han C, Zhang D, Zhang L, Liu B, Gao H, Zeng J, Zhou Y, Qiu Y, Wei J, Luo Y, Zhu F, Li X, Wu Q, Li B, Fu W, Tong Y, Meng J, Fang Y, Dong J, Feng Y, Xie S, Yang Q, Yang H, Wang Y, Zhang J, Gu H, Xuan H, Zou G, Luo C, Huang L, Yang B, Dong Y, Zhao J, Han J, Zhang X and Huang H. Majorbio Cloud: a one-stop, comprehensive bioinformatic platform for multiomics analyses. *iMeta* 2022; 1: e12.
- [16] Yachida S, Mizutani S, Shiroma H, Shiba S, Nakajima T, Sakamoto T, Watanabe H, Masuda K, Nishimoto Y, Kubo M, Hosoda F, Rokutan H, Matsumoto M, Takamaru H, Yamada M, Matsuda T, Iwasaki M, Yamaji T, Yachida T, Soga T, Kurokawa K, Toyoda A, Ogura Y, Hayashi T, Hatakeyama M, Nakagama H, Saito Y, Fukuda S, Shibata T and Yamada T. Metagenomic and metabolomic analyses reveal distinct stage-specific phenotypes of the gut microbiota in colorectal cancer. *Nat Med* 2019; 25: 968-976.
- [17] Zuo HL, Huang HY, Lin YC, Liu KM, Lin TS, Wang YB and Huang HD. Effects of natural products on enzymes involved in ferroptosis: regulation and implications. *Molecules* 2023; 28: 7929.
- [18] Song X and Long D. Nrf2 and ferroptosis: a new research direction for neurodegenerative diseases. *Front Neurosci* 2020; 14: 267.
- [19] Olayanju A, Coppie IM, Bryan HK, Edge GT, Sison RL, Wong MW, Lai ZQ, Lin ZX, Dunn K, Sanderson CM, Alghanem AF, Cross MJ, Ellis EC, Ingelman-Sundberg M, Malik HZ, Kitteringham NR, Goldring CE and Park BK. Brusatol provokes a rapid and transient inhibition of Nrf2 signaling and sensitizes mammalian cells to chemical toxicity-implications for therapeutic targeting of Nrf2. *Free Radic Biol Med* 2015; 78: 202-212.
- [20] Winterhoff M, Chen F, Sahini N, Ebensen T, Kuhn M, Kaever V, Bähre H and Pessler F. Establishment, validation, and initial application of a sensitive LC-MS/MS assay for quantification of the naturally occurring isomers itaconate, mesaconate, and citraconate. *Metabolites* 2021; 11: 270.
- [21] Chen F, Elgaher WAM, Winterhoff M, Büssow K, Waqas FH, Graner E, Pires-Afonso Y, Casares Perez L, de la Vega L, Sahini N, Czichon L, Zobl W, Zillinger T, Shehata M, Pleschka S, Bähre H, Falk C, Michelucci A, Schuchardt S, Blankenfeldt W, Hirsch AKH and Pessler F. Citraconate inhibits ACOD1 (IRG1) catalysis, reduces interferon responses and oxidative stress, and modulates inflammation and cell metabolism. *Nat Metab* 2022; 4: 534-546.
- [22] Zhu J, Djukovic D, Deng L, Gu H, Himmati F, Abu Zaid M, Chiorean EG and Rafferty D. Targeted serum metabolite profiling and sequential metabolite ratio analysis for colorectal cancer progression monitoring. *Anal Bioanal Chem* 2015; 407: 7857-7863.

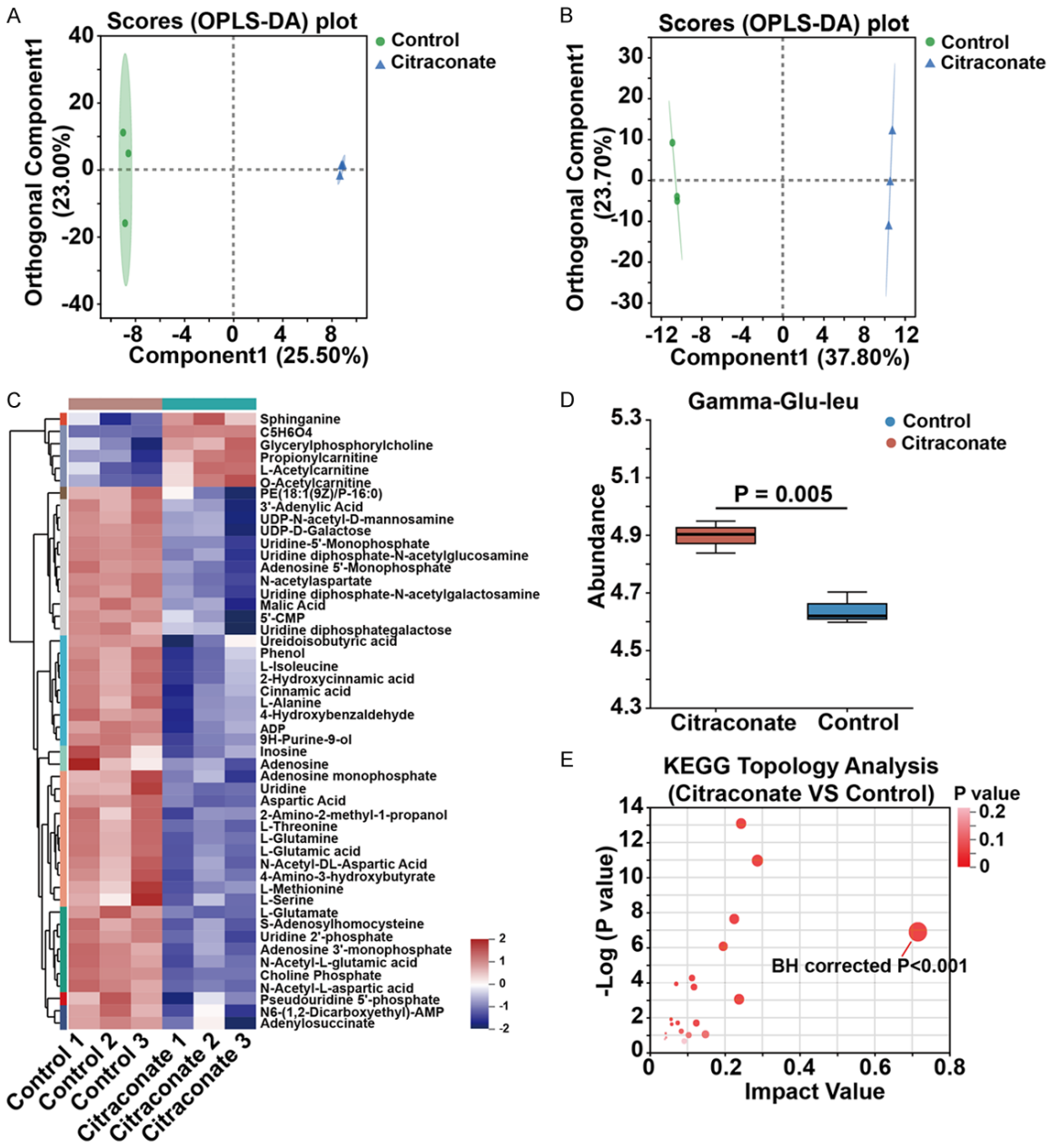
Citraconate aggravates colorectal cancer progression

- [23] Kang YP, Mockabee-Macias A, Jiang C, Falzone A, Prieto-Farigua N, Stone E, Harris IS and DeNicola GM. Non-canonical glutamate-cysteine ligase activity protects against ferroptosis. *Cell Metab* 2021; 33: 174-189, e177.
- [24] Chen X, Li J, Kang R, Klionsky DJ and Tang D. Ferroptosis: machinery and regulation. *Autophagy* 2021; 17: 2054-2081.
- [25] Bystrom LM, Guzman ML and Rivella S. Iron and reactive oxygen species: friends or foes of cancer cells? *Antioxid Redox Signal* 2014; 20: 1917-1924.
- [26] Wei R, Zhao Y, Wang J, Yang X, Li S, Wang Y, Yang X, Fei J, Hao X, Zhao Y, Gui L and Ding X. Tagitinin C induces ferroptosis through PERK-Nrf2-HO-1 signaling pathway in colorectal cancer cells. *Int J Biol Sci* 2021; 17: 2703-2717.
- [27] Latunde-Dada GO. Ferroptosis: role of lipid peroxidation, iron and ferritinophagy. *Biochim Biophys Acta Gen Subj* 2017; 1861: 1893-1900.
- [28] Del Rio D, Stewart AJ and Pellegrini N. A review of recent studies on malondialdehyde as toxic molecule and biological marker of oxidative stress. *Nutr Metab Cardiovasc Dis* 2005; 15: 316-328.
- [29] Chen C, Yang Y, Guo Y, He J, Chen Z, Qiu S, Zhang Y, Ding H, Pan J and Pan Y. CYP1B1 inhibits ferroptosis and induces anti-PD-1 resistance by degrading ACSL4 in colorectal cancer. *Cell Death Dis* 2023; 14: 271.
- [30] Lei S, Chen C, Han F, Deng J, Huang D, Qian L, Zhu M, Ma X, Lai M, Xu E and Zhang H. AMER1 deficiency promotes the distant metastasis of colorectal cancer by inhibiting SLC7A11- and FTL-mediated ferroptosis. *Cell Rep* 2023; 42: 113110.
- [31] Li D and Li Y. The interaction between ferroptosis and lipid metabolism in cancer. *Signal Transduct Target Ther* 2020; 5: 108.
- [32] Liu X, Zhang Y, Wu X, Xu F, Ma H, Wu M and Xia Y. Targeting ferroptosis pathway to combat therapy resistance and metastasis of cancer. *Front Pharmacol* 2022; 13: 909821.
- [33] Zhang R, Chen J, Wang S, Zhang W, Zheng Q and Cai R. Ferroptosis in cancer progression. *Cells* 2023; 12: 1820.
- [34] Li Y, Tuerxun H, Liu X, Zhao Y, Wen S, Li Y, Cao J and Zhao Y. Nrf2—a hidden bridge linking cancer stem cells to ferroptosis. *Crit Rev Oncol Hematol* 2023; 190: 104105.
- [35] Liu C, Wang G, Han W, Tian Q and Li M. Ferroptosis: a potential therapeutic target for stroke. *Neural Regen Res* 2024; 19: 988-997.
- [36] Trujillo J, Chirino YI, Molina-Jijón E, Andérica-Romero AC, Tapia E and Pedraza-Chaverrí J. Renoprotective effect of the antioxidant curcumin: recent findings. *Redox Biol* 2013; 1: 448-456.
- [37] Forcina GC and Dixon SJ. GPX4 at the crossroads of lipid homeostasis and ferroptosis. *Proteomics* 2019; 19: e1800311.
- [38] Liu Y, Wan Y, Jiang Y, Zhang L and Cheng W. GPX4: the hub of lipid oxidation, ferroptosis, disease and treatment. *Biochim Biophys Acta Rev Cancer* 2023; 1878: 188890.
- [39] Nguyen KA, Conilh L, Falson P, Dumontet C and Boumendjel A. The first ADC bearing the ferroptosis inducer RSL3 as a payload with conservation of the fragile electrophilic warhead. *Eur J Med Chem* 2022; 244: 114863.
- [40] Singhal R, Mitta SR, Das NK, Kerk SA, Sajjakulnukit P, Solanki S, Andren A, Kumar R, Olive KP, Banerjee R, Lyssiotis CA and Shah YM. HIF-2 α activation potentiates oxidative cell death in colorectal cancers by increasing cellular iron. *J Clin Invest* 2021; 131: e143691.
- [41] Luo Y, Huang S, Wei J, Zhou H, Wang W, Yang J, Deng Q, Wang H and Fu Z. Long noncoding RNA LINC01606 protects colon cancer cells from ferroptotic cell death and promotes stemness by SCD1-Wnt/ β -catenin-TFE3 feedback loop signalling. *Clin Transl Med* 2022; 12: e752.
- [42] Ye S, Xu M, Zhu T, Chen J, Shi S, Jiang H, Zheng Q, Liao Q, Ding X and Xi Y. Cytochrome promotes sensitivity to ferroptosis by regulating p53-YAP1 axis in colon cancer cells. *J Cell Mol Med* 2021; 25: 3300-3311.
- [43] He F, Ru X and Wen T. NRF2, a transcription factor for stress response and beyond. *Int J Mol Sci* 2020; 21: 4777.
- [44] Dodson M, Castro-Portuguez R and Zhang DD. NRF2 plays a critical role in mitigating lipid peroxidation and ferroptosis. *Redox Biol* 2019; 23: 101107.
- [45] Mills EL, Ryan DG, Prag HA, Dikovskaya D, Menon D, Zaslona Z, Jedrychowski MP, Costa ASH, Higgins M, Hams E, Szpyt J, Runtsch MC, King MS, McGouran JF, Fischer R, Kessler BM, McGettrick AF, Hughes MM, Carroll RG, Booty LM, Knatko EV, Meakin PJ, Ashford MLJ, Modis LK, Brunori G, Sévin DC, Fallon PG, Caldwell ST, Kunji ERS, Chouchani ET, Frezza C, Dinkova-Kostova AT, Hartley RC, Murphy MP and O'Neill LA. Itaconate is an anti-inflammatory metabolite that activates Nrf2 via alkylation of KEAP1. *Nature* 2018; 556: 113-117.

Citraconate aggravates colorectal cancer progression

Table S1. Primers for qPCR

Gene name	Forward primer (5'-3')	Reverse primer (5'-3')
<i>GAPDH</i> (human)	TGTTGCCATCAATGACCCCTT	CTCCACGACGACTACTCAGCG
<i>NQO1</i> (human)	TGGTGGAGTCGGACCTCTATGC	GTCTGCGGCTTCCAGCTTCTT
<i>GCLC</i> (human)	AGTCCGGTTGGTCTGTCTG	GCTGTCTGGTGTCCCTTCA
<i>GCLM</i> (human)	TCTTGCCTCCTGCTGTGTGA	CCACTCGTGCCTTGAATGT
<i>NFE2L2</i> (human)	TTCTTCAGCAGCATCCTCTCC	TCTGTGTGACTGTGGCATCTG
<i>Gapdh</i> (mouse)	AAGGTGGTGAAGCAGGCATCT	AAGGTGGTGAAGCAGGCATCT
<i>Nqo1</i> (mouse)	GGTAGCGGCTCCATGACTCTC	GCAGGATGCCACTCTGAATCG
<i>Gclc</i> (mouse)	GCCTGGAGCCTCTGAAGAACA	CGTGCTGTGCCAGAAGATGATC
<i>Gclm</i> (mouse)	CGTGCTGTGCCAGAAGATGATC	GCTGCTCCAACCTGTGCTTGTGC



Citraconate aggravates colorectal cancer progression

Figure S1. Citraconate regulates glutamate metabolism. (A) LC-MS were performed on HCT116 cells treated with 12 mM citraconate for 24 hours. OPLS-DA achieved a fairly distinct separation in positive (A) and negative (B) ion modes. (C) Cluster analysis of differential metabolites showed that the contents of L-glutamic acid and L-glutamine decreased in the citraconate treatment group. (D) γ -glutamyl peptide synthesis increased in HCT116 cells treated with citraconate. (E) KEGG topological analysis based on differential metabolites.

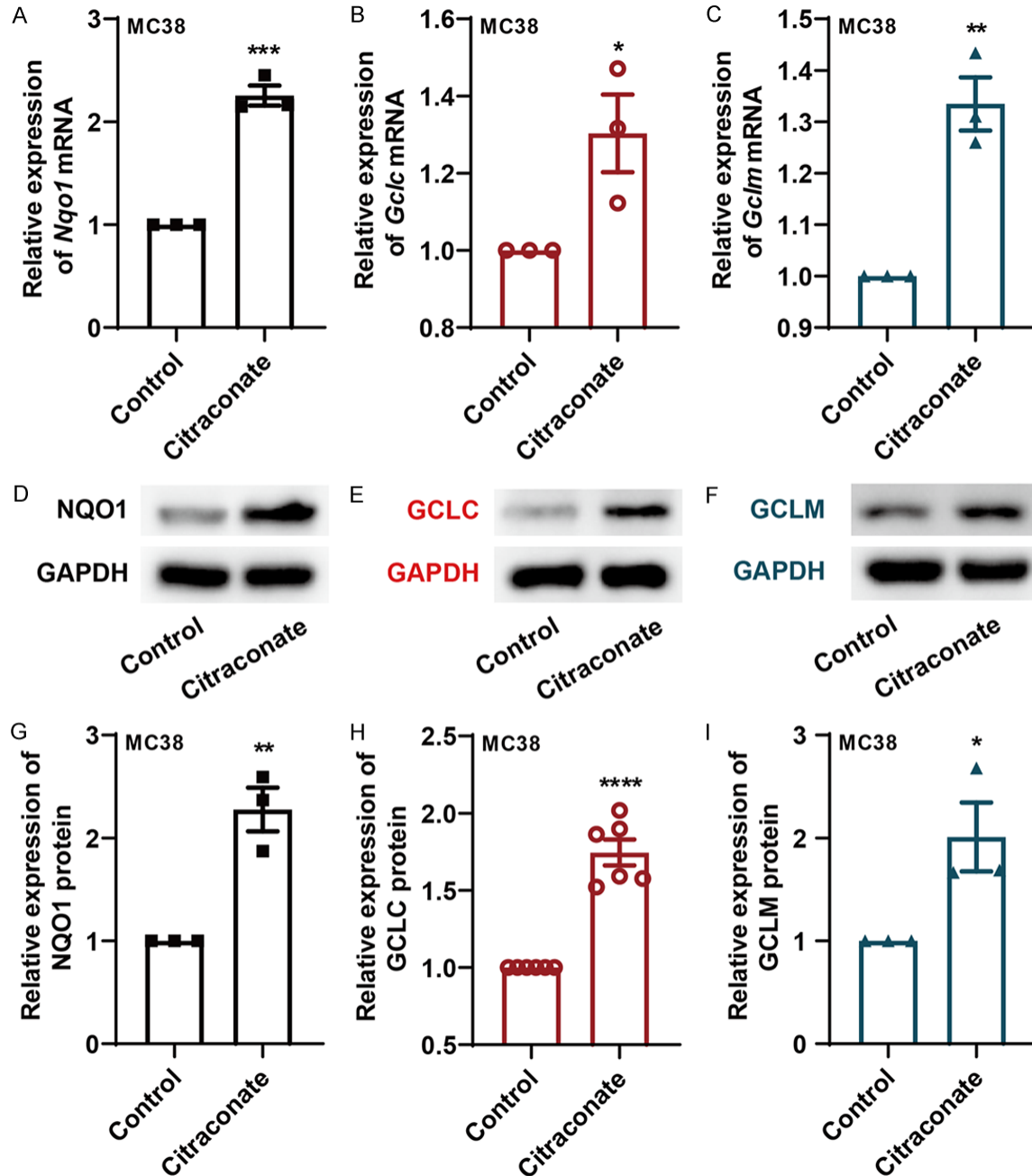


Figure S2. Citraconate up-regulates the expression of ferroptosis suppressor genes in MC38 cells. *Nqo1* (A), *Gclc* (B), and *Gclm* (C) mRNA were detected by qRT-PCR after MC38 cells were treated with 9 mM citraconate for 24 hours. Protein expression of NQO1 (D, G), GCLC (E, H), and GCLM (F, I) was detected by western blot after MC38 cells were treated with 9 mM citraconate for 48 hours. Experiments were repeated at least three times. Unpaired two-tailed Student's *t* test was used for comparisons between the two groups. Data were presented as Mean \pm SEM. * $P < 0.05$, ** $P < 0.01$, **** $P < 0.0005$.

Citraconate aggravates colorectal cancer progression

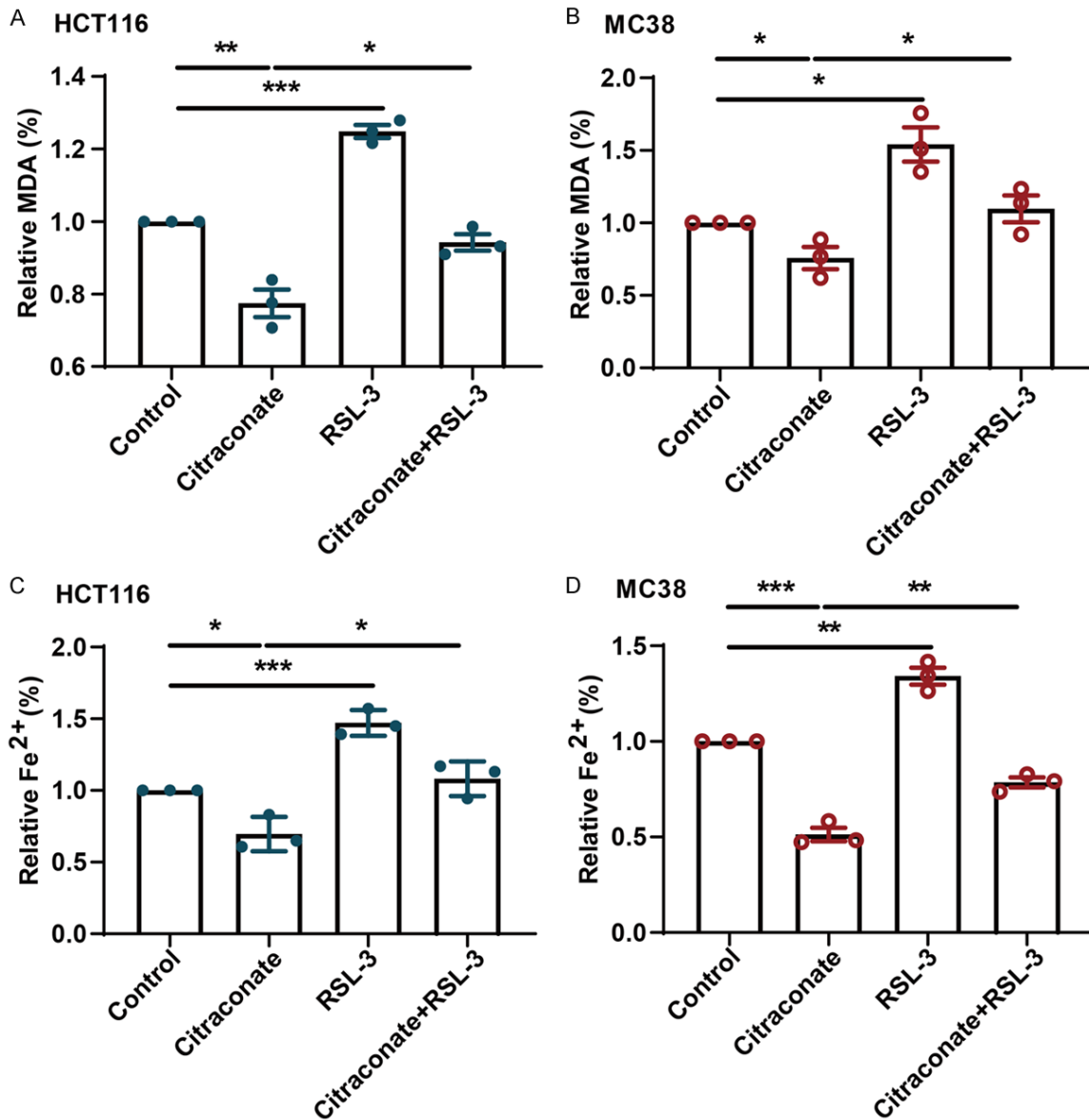


Figure S3. RSL3 induces ferroptosis in colorectal cancer cells. HCT116 and MC38 cells were pre-treated with 1 μ M RSL3 and 0.5 μ M RSL3 for 2 hours, respectively. Next, treatment groups were incubated with 12 mM citraconate, 1 μ M RSL3, or both of them for 72 hours in HCT116 cells. And treatment groups were incubated with 9 mM citraconate, 0.5 μ M RSL3, or both of them for 48 hours in MC38 cells. The cellular MDA and ferrous iron levels were assessed in HCT116 (A, C) and MC38 (B, D) cells. Experiments were repeated at least three times. Unpaired two-tailed Student's *t* test was used for comparisons between the two groups. Data were presented as Mean \pm SEM. ns stands for no significance. **P*<0.05, ***P*<0.01, ****P*<0.005.

Citraconate aggravates colorectal cancer progression

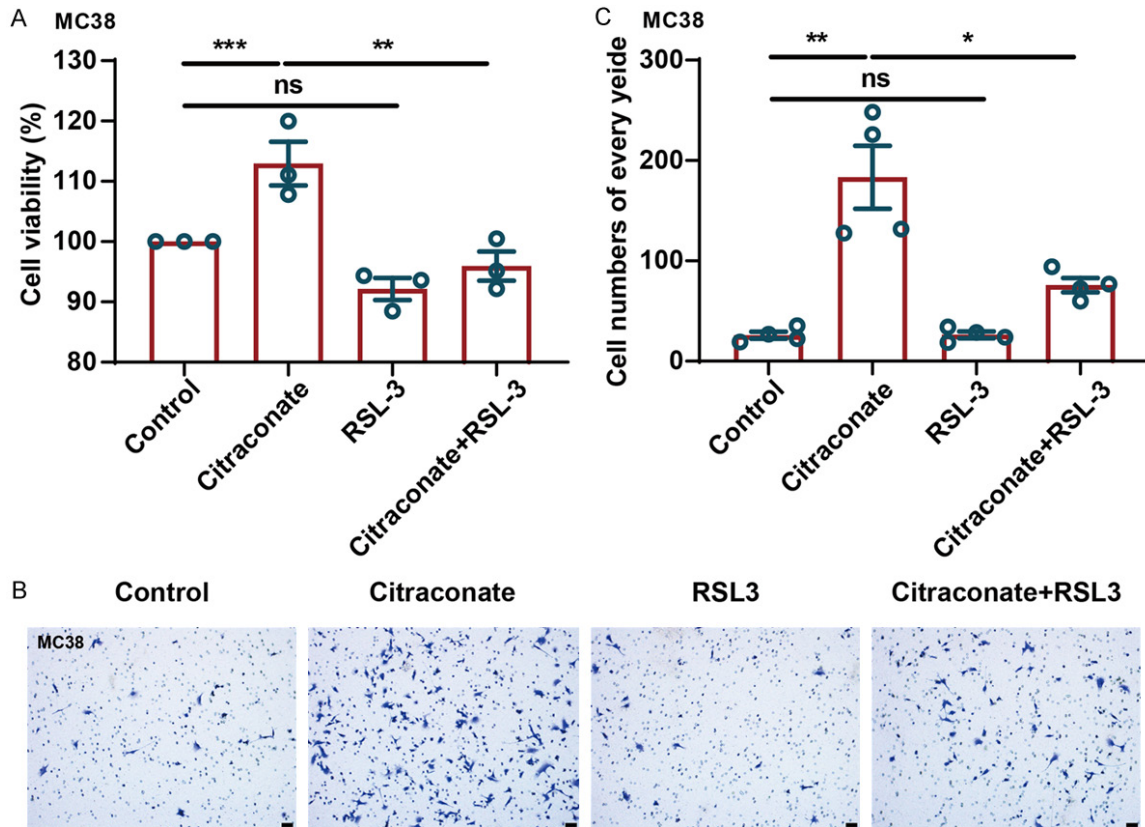


Figure S4. Citraconate inhibits ferroptosis in MC38 cells. **A.** MC38 cells were incubated with 9 mM citraconate with or without 0.1 μ M RSL3 for 48 hours. Then, cell viability was measured by Cell Counting Kit-8 assay. After 1.2×10^5 MC38 cells seeded in the transwell chamber for 6 hours, the cells were pre-treated with 0.5 μ M RSL3 for 2 hours. Next, treatment groups were incubated with 9 mM citraconate, 0.5 μ M RSL3, or both of them for 16 hours, respectively. **B.** Representative images of migrating cells stained with crystal violet were displayed. Scale bars: 50 μ m in black. **C.** Quantitative analysis for the number of migrating cells. Experiments were repeated at least three times. Unpaired two-tailed Student's *t* test was used for comparisons between the two groups. Data were presented as Mean \pm SEM. ns stands for no significance. **P*<0.05, ***P*<0.01, ****P*<0.005.